

DOI: <https://doi.org/10.24297/jap.v16i1.8274>

MWCNTs/ZnO Nanofibers Fabrication, Properties and Applications

M. Dawy and Rabab Khaled

Department of Physical Chemistry, National Research Center, Giza, 12622, Egypt.

m_dawy9@yahoo.com

Abstract

Electrospun MWCNTs nanofibers (CNF1, CNF2 and CNF3) with different concentrations of MWCNTs (0.3, 1.5, 2 wt%), respectively, were deposited on Aluminum foil substrates. Also, Zinc Acetate dihydrate $Zn(CH_3COO)_2 \cdot 2H_2O$ (ZNF) and MWCNTs/zinc acetate (CZNF) nanofibers were deposited on Aluminum foil substrates and annealed in the presence of oxygen at 400 °C. The resultant fibers were characterized using X-ray diffraction (XRD), scanning electron microscope with energy dispersive X-Ray spectrophotometry (SEM, EDX), Fourier transform infrared (FTIR). SEM, EDX and FTIR exhibited a total decomposition of the organic precursor after calcination and formation of zinc oxide (ZONF and CZONF). The mean fiber diameter was found to be increased with increasing MWCNTs concentration and ranged 490-767 nm. XRD patterns indicated that ZnO was corundum with the hexagonal wurtzite structure. The crystallite size of ZONF and CZONF were determined by shurrer equation to be 26 and 29.7 nm, respectively. The optical analysis indicated that the percentage transmittance increased after calcination. The band gap for the electrospun fibers before and after calcination was calculated. CZONF nanofibers have electrical properties similar to those of semiconductors. The tested compounds CNF2, CNF3, CZNF and CZONF exhibited different activities against the bacteria and yeast pathogen *Candida albicans*. CZNF compound is the most active against the bacteria and yeast pathogen. So, these compounds can be used as food packaging.

Keywords

MWCNTs/ZnO Nanofibers, electrical, optical and biological properties

1. Introduction

Carbon nanotubes (CNTs) have attracted considerable research interest in the last decade because of their unique optical, electronic, magnetic, mechanical, and gas adsorption properties. They have been regarded as promising candidates for versatile applications. Exhibiting high electrical conductivity and high electron storage capacity (one electron for every 32 carbon atoms) [1, 2], CNTs can act as extremely effective electron sinks. Hence, CNTs supported with metal oxide nanoparticles are expected to exhibit different physical properties from those of neat CNT.

Zinc oxide semiconductor materials have been widely used primarily due to low cost and outstanding chemical and physical properties [3]. ZnO is an n-type material having a wide band gap (3.21–3.42 eV) at room temperature. It is a group II–VI compound semiconductor having a stable wurtzite structure and large excitation binding energy of 60 meV with lattice spacing $a = 0.325$ nm and $c = 0.521$ nm. It is a unique material that exhibits optical, semiconducting, pyroelectric and piezoelectric properties [4,5]. It has attracted serious research attention because of its applicability to wide applications such as light emitting diode, [6, 7], solar cells [8, 9], chemical and gas sensors [10], ultraviolet (UV) light detector [11], stimulated emission with low loss and high gain [12], and transparent conducting oxide [13]. Due to these varied applications, several methods including thin films and polymeric approaches have been employed to deposit ZnO. Some of the thin film methods used include; chemical vapour deposition [14,15,16], chemical bath deposition [17], laser deposition [18,19].

ZnO nanoparticles have exhibited a strong bacterial growth inhibiting character [20]. ZnO has also gathered significant attention due to its various applications such as UV light emitting diodes, laser diodes and catalysts [21]. ZnO is widely used to treat a variety of skin conditions, in products such as baby powder, barrier creams to treat diaper rashes and in Calamine lotion, antidandruff shampoos and antiseptic ointments [22]. Nano zinc is non-toxic, with wide band gap has also been identified as a promising semiconductor material for exhibiting ferromagnetism (RFTM) at room temperature when doped with most of the transition metal elements [23].

The electrospinning method dates back to the work of Zeleny in 1914 and was previously termed "electrostatic spinning". This researcher found the technique to be useful for spinning polymer fibers having a small diameter [24]. This method, which uses the principle of electrostatics depends on electromotive force to form a fiber. This method has also been described as indispensable in the scientific and economic resurgence for developing nations [25]. Electrospinning has continued to gain serious research attention owing to its unique properties of the resultant nano/micro fibres (large surface area to volume ratio and cost effectiveness) [26, 27]. ZnO nanofibres, including nanotube and nanorods [28] belong to the one-dimensional group of nanomaterials which are flexible in nature. ZnO nanofibres have demonstrated improved properties in photoconducting, semi-conducting and piezoelectric properties [29, 30 & 31].

In this study, we synthesized ZnO and ZnO/MWCNTs nanofibers by electrospinning technique. The fibers have been characterized for morphology, composition, structure and further investigated for the antibacterial properties with respect to their crystallite size. Also, dielectric constant and conductivity will be studied. The nanofiber Such a material was designed and synthesized with a view to electronic and biological applications.

2. Materials and Methods

MWCNT, nitric acid (68% conc), ethanol, Poly(vinyl Alcohol) (Mw = 125,000 g by GPC), zinc acetate dihydrate ($\text{Zn}(\text{CH}_3\text{COO})_2 \cdot 2\text{H}_2\text{O}$) salt $\geq 99\%$ assay from Sigma-Aldrich.

Experimental

Modification of MWCNT:

0.5 gm of MWCNT was dissolved in 63 ml nitric acid (68% conc) and completed with distilled water till 100 ml. The solution was refluxed for 20 h and 100°C . The precipitate was washed with ethanol and distilled water several times up to pH value of 7 and was dried at 70°C .

Preparation of MWCNT nanofibers:

Different weight percent of MWCNT (0.3, 1.5, 2 wt%) was dissolved in ethanol and sonicated for 1 h, then different weight percent of PVA (13 and 20 wt%) (dissolved in distilled H_2O at $50\text{-}60^\circ\text{C}$) was added and stirring for 30 min. The prepared solution was fed into the spinneret. The distance between the tip of the spinneret and the substrate was kept at 12 cm. 16 kV voltage was applied to the solution and the substrate attached to an aluminium foil was grounded. The produced nanofibers were put in the drier at 50°C .

Preparation of ZnO_2 nanofibers:

10 wt% zinc acetate was dissolved in distilled H_2O , then 30 wt% PVA was added and stirring for 30 min. The prepared solution was fed into the spinneret. The distance between the tip of the spinneret and the substrate was kept at 12 cm. 16 kV voltage was applied to the solution and the substrate attached to an aluminium foil was grounded. The produced nanofibers were put in the drier at 50°C . The deposited fibres were calcined at 400°C in furnace in the presence of oxygen for 4h.

Preparation of MWCNT -ZnO₂nanofibers:

0.5 wt% MWCNT was dissolved in ethanol and sonication for 2h, then 10 wt% zinc acetate (dissolved in distilled H₂O) was added and stirring for 30 min. Finally, 20wt% PVA was added and stirring for 30 min. The prepared solution was fed into the spinneret. The distance between the tip of the spinneret and the substrate was kept at 12 cm. 16 kV voltage was applied to the solution and the substrate attached to an aluminium foil was grounded. The produced nanofibers were put in the drier at 50 °C. The deposited fibres were calcined at 400°C in furnace in the presence of oxygen for 4h [32].

Table 1: The codes of the prepared samples

Code	MWCNTs	Zinc acetate	PVA
MWCNTs nanofibers 1 (CNF1)	0.3 wt%	-	13 wt%
MWCNTs nanofibers 2 (CNF2)	1.5 wt%	-	20 wt%
MWCNTs nanofibers 3 (CNF3)	2 wt%	-	20 wt%
Zinc acetate nanofibers (ZNF)	-	10 wt%	30 wt%
Zinc oxide nanofibers after calcination of ZNF (ZONF)	-	-	-
MWCNTs-zinc acetate nanofibers (CZNF)	0.5 wt%	10 wt%	20 wt%
MWCNTs-zinc oxide nanofibers after calcination of CZNF (CZONF)			

Antimicrobial Assay

The antimicrobial activities of samples were determined by the agar diffusion technique [33]. Sterile nutrient and Czapek'sdiox agar media were inoculated, separately, with 100 µl cell suspension of the tested bacteria and yeast poured into Petri-dishes (15 cm diameter). Each sample was dissolved in dimethyl sulfoxide (DMSO) with concentration (10 mg/ml), 50 µl from each sample was bearing on filter paper disc (1 cm diameter). Solvent was allowed to evaporate and the discs were deposited on the surface of inoculated agar plates and kept at low temperature before incubation which favors diffusion over microbial growth to detect the inhibition zone clearly. The plates were incubated at 35°C for bacteria and at 30°C for yeast. The antimicrobial activity was expressed as the diameter of inhibition zone in mm and compared with the antibiotic amoxicillin trihydrate.

Measurements:

The as-spun and calcined fibres were analysed for their chemical, structural, optical and electrical properties. Scanning electron microscopy (SEM) observations were carried out using a QUANTA FEG250 field emission scanning electron microscope. X-ray diffraction (XRD) measurements were performed using Philips PW 1710 diffractometer with Cu K radiation. The energy dispersive X-ray (EDAX) analysis provides a way of analysing the chemical composition of the prepared materials. Dielectric parameters were recorded in the frequency range (100 HZ-5 MHZ) using HIOKI Japan 3532-50 LCR HI TESTER.

3. Results and Discussion:

3.1. XRD analysis:

XRD patterns of as-prepared nanofibers samples were studied to investigate its crystal structure. Fig.1 showed the XRD patterns of ZNF and CZNF. ZNF exhibited lower intensity peaks due to lower crystallinity since the material is amorphous. Whereas in CZNF, the distributions of prominent diffraction peaks matched well with rhombohedral structure of graphite structure derived from [34].

It can be noticed that, XRD patterns (Fig.2) of ZONF and CZONF exhibited polycrystalline nature consisting of several diffraction peaks of hexagonal wurtzite structure with major five diffraction peaks at $2\theta = 31.85^\circ, 34.52^\circ, 36.37^\circ, 47.52^\circ$ and 56.69° , respectively, pertaining to (100), (002), (101), (102) and (110) planes of ZnO. All diffraction peaks are in good agreement with those of the structure of ZnO (**JCPDS card 96-230-0113**) [34]. The unit cell parameters of the ZnO were found to be $a = 3.2494 \text{ \AA}$ and $c = 5.2054 \text{ \AA}$ [35]. The appearance of the characteristic ZnO peak pattern clearly showed that PVA is decomposed and the nanofibers are composed of ZnO. XRD pattern of CZONF showed broadening of the peaks and this confirmed that the composite contains MWCNTs. The average crystallite size of ZONF and CZONF calculated using the Debye–Scherrer equation:

$$d = k\lambda / \beta \cos\theta$$

where d is the average crystal size of particles, k is the Debye–Scherrer constant (0.9), λ is the Xray wavelength (0.15406 nm), β is the line broadening in a radian obtained from the full width at half maximum, and θ is the Bragg angle. The average crystal size of ZONF and CZONF were found to be 26 and 29.7 nm, respectively.

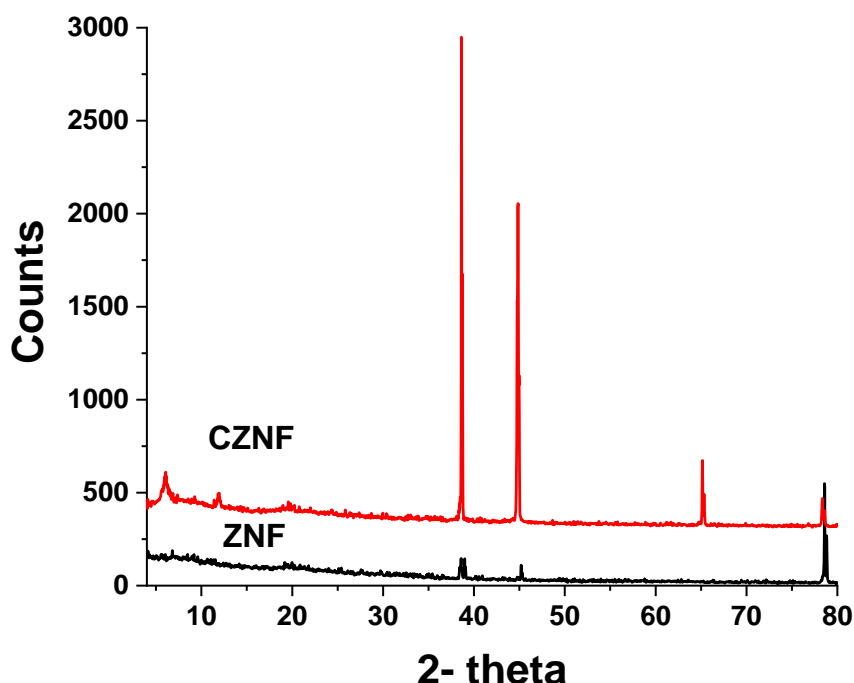


Fig.1: XRD patterns of zinc acetate nanofibers (ZNF) and MWCNTs-zinc acetate nanofibers (CZNF).

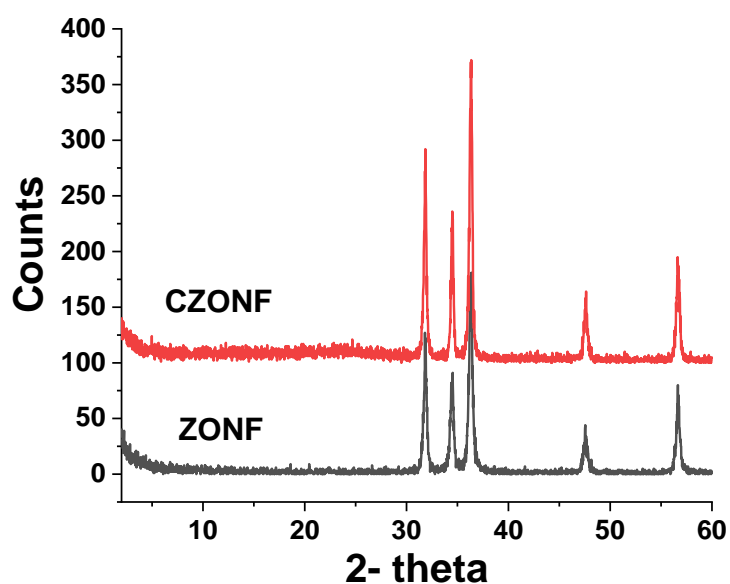
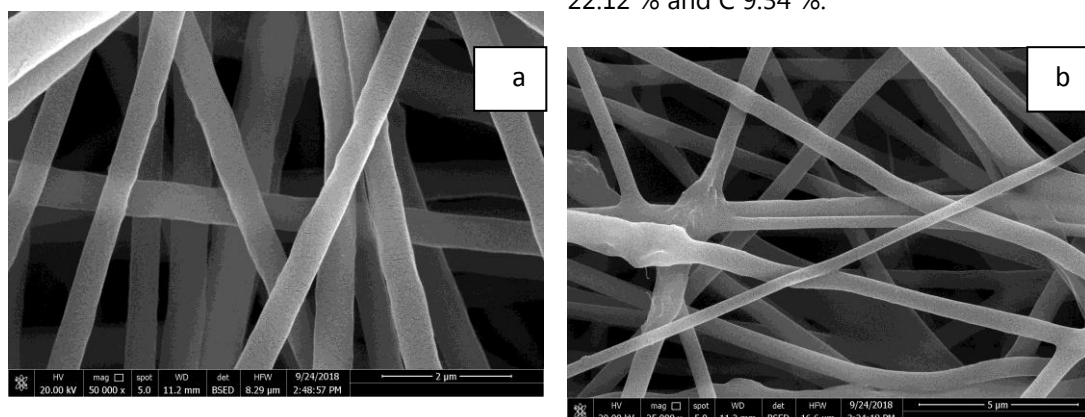


Fig.2: XRD patterns of zinc oxide nanofibers (ZONF) and MWCNTs-zinc oxide nanofibers (CZONF) after calcination.

3.2. SEM:

Fig.3. showed SEM images of CNF1, CNF2, CNF3, ZNF and CZNF. The average fiber diameter was found to be increased from 490 to 767 nm with increasing the concentration of MWCNTs.

SEM images of ZONF and CZONF after calcination were shown in Fig.4. It can be noticed that, the deposited nanofibers were non-woven in nature and are bead free. The difference in the measured mean fiber diameter observed in the as-spun and calcined materials could be attributed to the removal of PVA which served as a carrier for the metal oxide and other volatile organic constituents, such as acetate, during the calcination process. The EDX analysis of the calcined CZONF was shown in Fig.5 and Table 2. It is evident from the spectra that the fibers contained the desired elements: Zn 68.54 % , O 22.12 % and C 9.34 %.



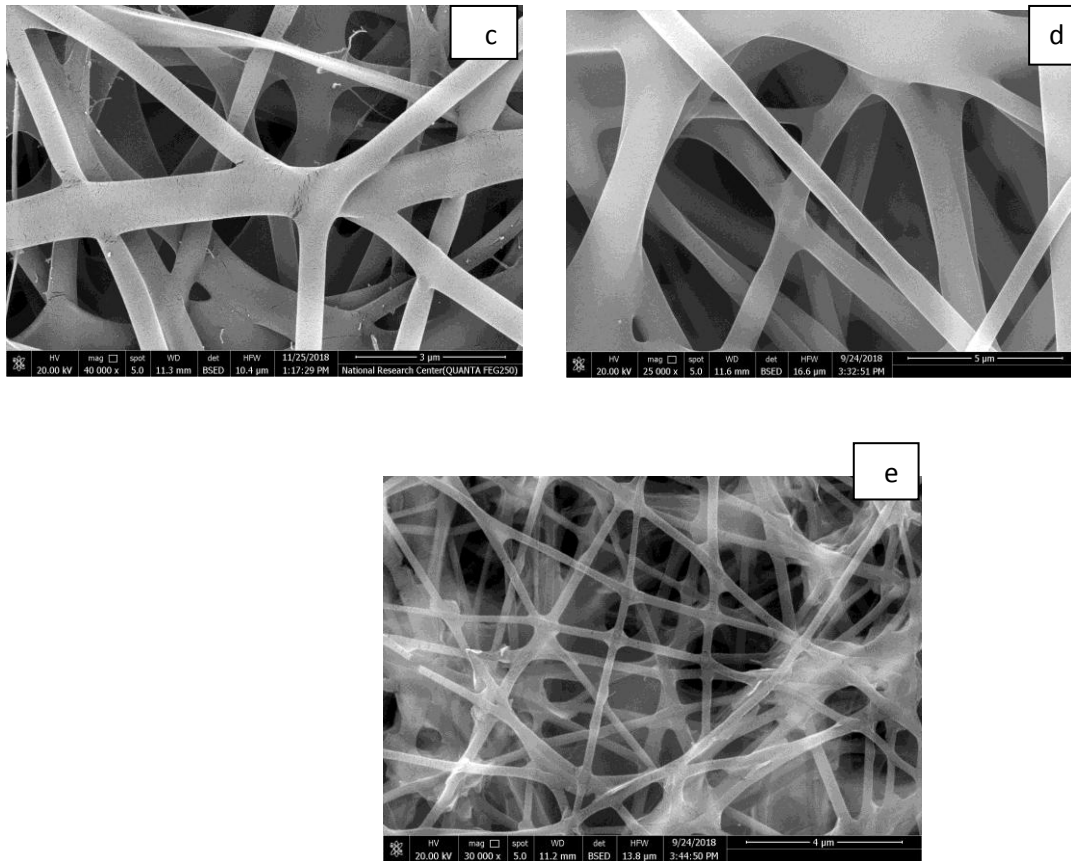


Fig.3: SEM images of (a) MWCNTs nanofibers (CNF1), (b) CNF2, (c) CNF3, (d) Zinc acetate nanofibers (ZNF), (e) MWCNTs-zinc acetate nanofibers (CZNF).

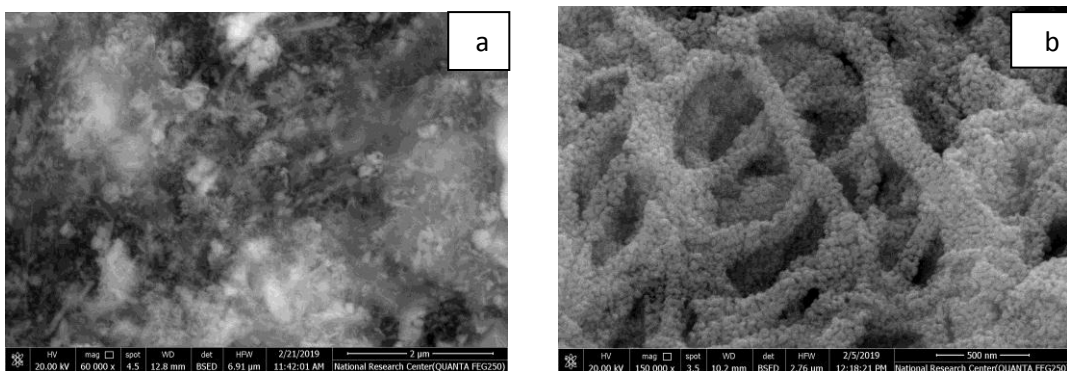
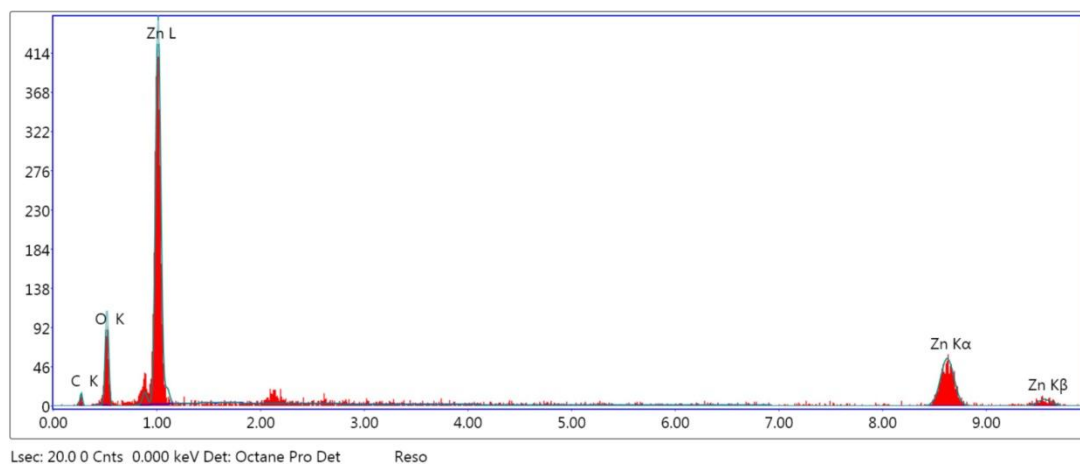


Fig.4: SEM images of (a) Zinc oxide nanofibers (ZONF) and (b) MWCNTs-zinc oxide nanofibers (CZONF) after calcination.



Element	Weight %	Atomic %	Net Int.	Error %
C K	9.34	24.24	2.19	29.11
O K	22.12	43.09	21.72	13.6
ZnK	68.54	32.67	42.85	7.38

Fig.5 and Table 2: Elemental composition of MWCNTs-zinc oxide nanofibers (CZONF) determined by EDAX

3.3. FT-IR

FT-IR examination was performed in the range 400-4000 cm^{-1} of the prepared samples to examine the detailed structure of the bonding. FT- IR spectra of different concentrations of MWCNTs. It can be seen that the intensity of the peaks increased with concentration of MWCNTs (Fig.6). However, after the MWCNTs are treated, many groups are introduced onto the surface of MWCNTs, such as carbonyl groups reveal at about 1705 cm^{-1} , and oxygen-hydrogen bonds and C=C bonds reveal at about 3427 cm^{-1} and 1568 cm^{-1} , respectively [36].

Fig.7 showed the FT-IR spectra of ZONF and CZONF calcined nanofibers. All the described peaks are weakened in the calcined ZnO nanofibers. Also, the calcined IR spectra showed a well defined peak of ZnO at 426 cm^{-1} , confirming the presence of ZnO and the decomposition of the PVA. Our results are in good agreement with the reported studies [37].

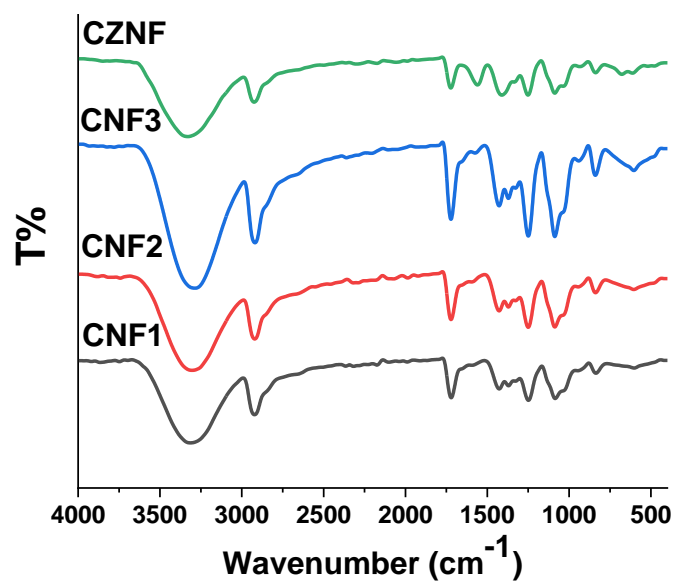


Fig.6: FT-IR spectra of MWCNTs nanofibers (CNF1), (CNF2), (CNF3) and MWCNTs-zinc acetate nanofibers (CZNF).

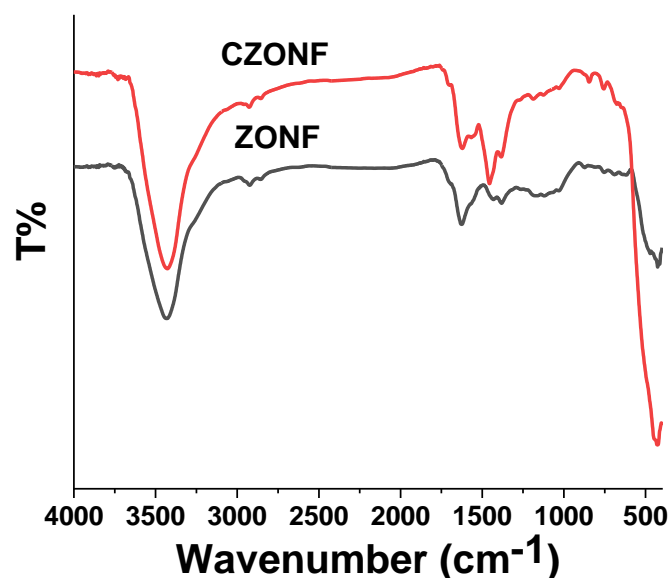


Fig.7: FT-IR spectra of zinc oxide nanofibers (ZNF) and MWCNTs-zinc oxide nanofibers (CZONF) after calcination.

Optical characterization:

UV-VIS transmittion:

An increase in the percent of transmittance was observed in Fig. 8 with increasing MWCNTs percent in the samples CNF1, CNF2 and CNF3 nanofibers. It can also be observed that the MWCNTs addition has a profound effect on the fiber's optical transparency; with increase in transparency down to 65% and great increase due to

the fact that the MWCNTs are not transparent and absorb the incoming light then increase the light scattering. Addition of Zn Acetate increased the transmittance in visible region to 80% percent. This can be revealed that the Zn-acetate fibers are highly transparent in the visible region from 600 nm about 95%.

After calcination of CZNF, the optical transmittance increases for CZONF compound. This finding could be attributed to the decomposition of all the organic components presents in the as-spun fibres and the transformation from the amorphous state to crystalline state as evidenced by the XRD results. The percent transmittance for CZNF (80%) was found to be lower than that of CZONF (90%). As earlier stated; the decomposition of the organic polymer and the removal of the acetate from the $\text{Zn}(\text{CH}_3\text{COO})_2 \cdot 2\text{H}_2\text{O}$ to form crystalline ZnO provoked a reduction in the thickness which led to a rise in the transmittance [38, 39]. The transmittance increased from the visible to the near-infrared region. A high transmittance value for zinc oxide was also reported previously, which implies that the ZnO deposited is very transparent as it allowed almost all the incident light to pass through it and absorbed very little as shown in Fig.9. The optical bandgap of the CZNF and CZONF was 1.56 and 2.75 eV and after calcination determined by assuming that ZnO is a direct band gap semiconductor

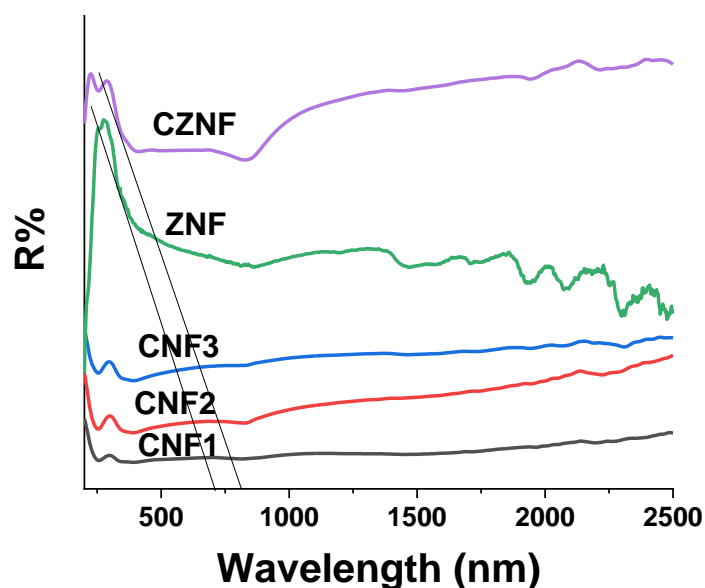


Fig.8: UV-VIS transmittance spectra of MWCNTs nanofibers, (CNF1), (CNF2), (CNF3) and MWCNTs/zinc acetate nanofibers (CZNF).

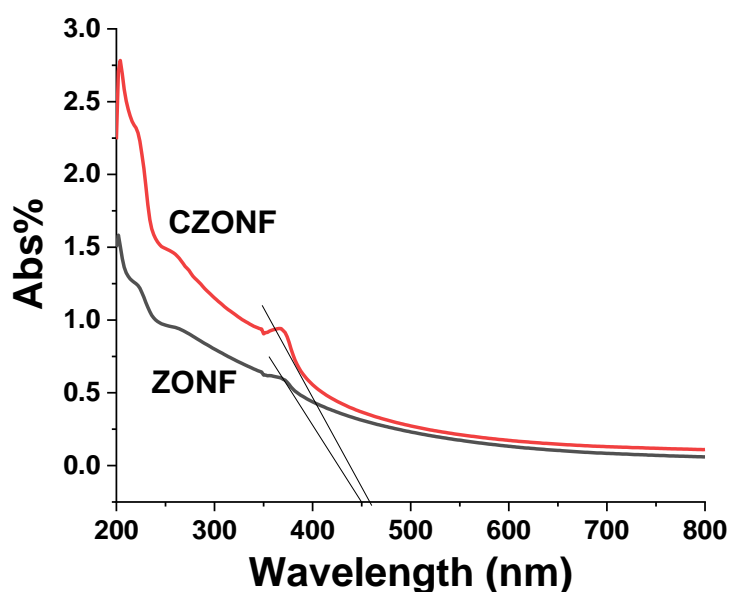


Fig.9: UV-VIS transmittion spectra of zinc oxide nanofibers (ZONF) and MWCNTs-zinc oxide nanofibers (CZONF) after calcination.

Table 3: the optical band gap of the samples

Nanocomposites	The band gap (ev)
ZNF	1.78
CZNF	1.56
ZONF	2.81
CZONF	2.75

Electrical Properties:

The change of the electrical properties (dielectric constant and conductivity) of CNF1, CNF2, CNF3, ZNF and CZNF according to different frequency and concentration of MWCNT were studied (Figs. 10-13). The dielectric constant (ϵ') of the MWCNTs nanofibers increased with increasing MWCNTs concentration whereas, ZNF is very low compared to that of CZNF individual MWCNTs.

The conductivity of ZNF is higher than that of CZNF, the reason for such low conductivity is that the presence of amorphous carbon and other impurities in MWCNTs prevents the flow of electrons [40-49]. One of the methods of improving the electrical properties of CNT fibers is to create a path through which electrons flow on the MWCNTs fibers [44, 45] succeeded in improving the electrical properties of MWCNT fibers via the synthesis of a metal-CNT composite fiber in a process called self-fuelled electrodeposition. Produced in such a way, the composite fibers were designed to serve as external circuits through which electrons could travel with a metal reductant deposited on the MWCNT surface. The electrical conductivity of CZNF nanocomposite fibers improved that of MWCNTs .

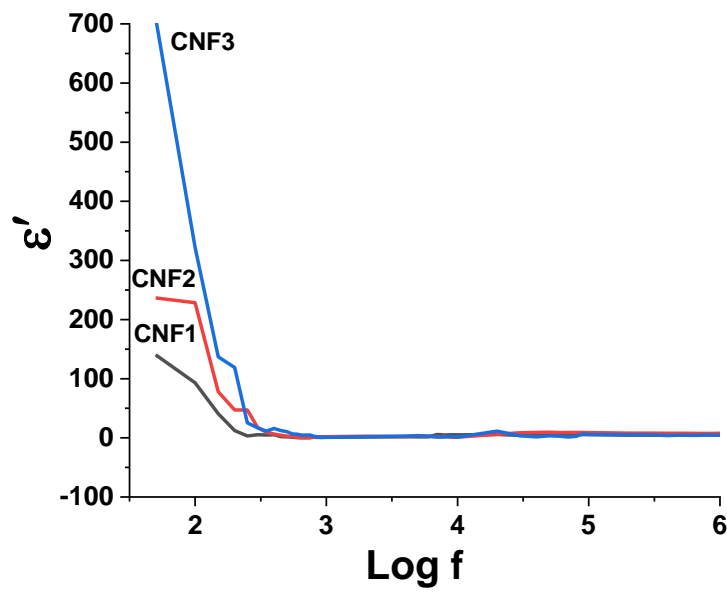


Fig.10: Variation of dielectric constant of MWCNTs nanofibers (CNF1), (CNF2) and (CNF3).

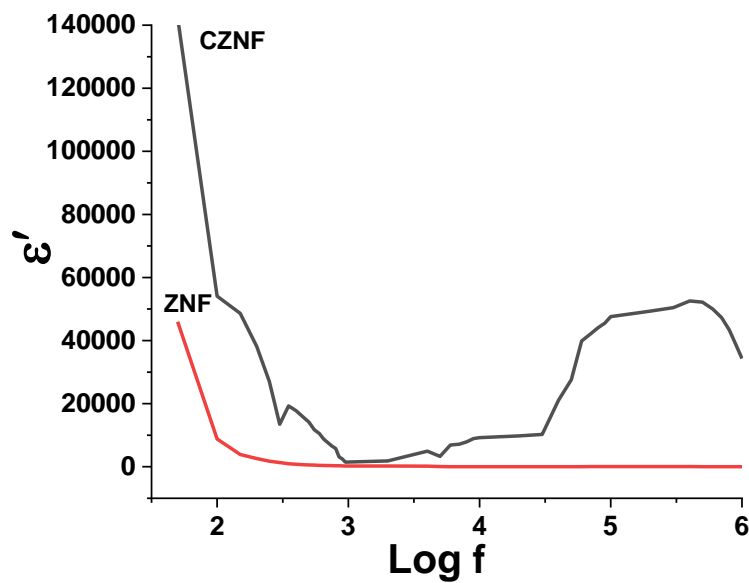


Fig.11: Variation of dielectric constant of zinc acetate nanofibers (ZNF) and MWCNTs-zinc acetate nanofibers (CZNF).

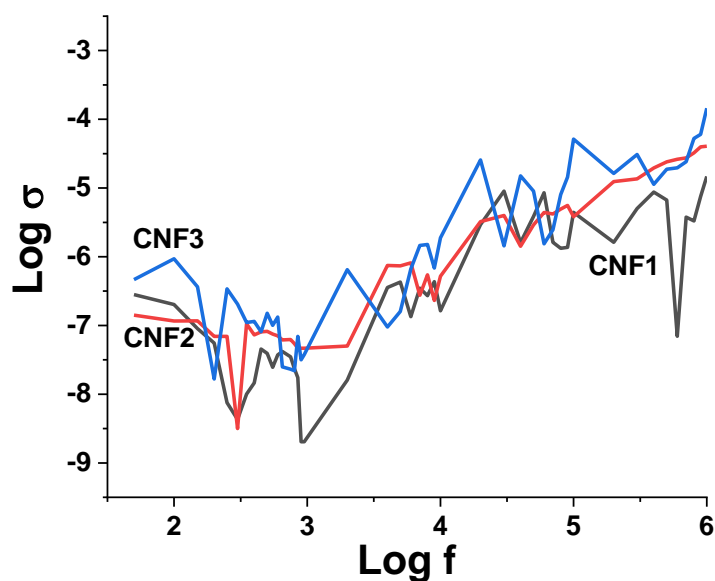


Fig.12: Variation of conductivity of MWCNTs nanofibers (CNF1), (CNF2) and (CNF3).

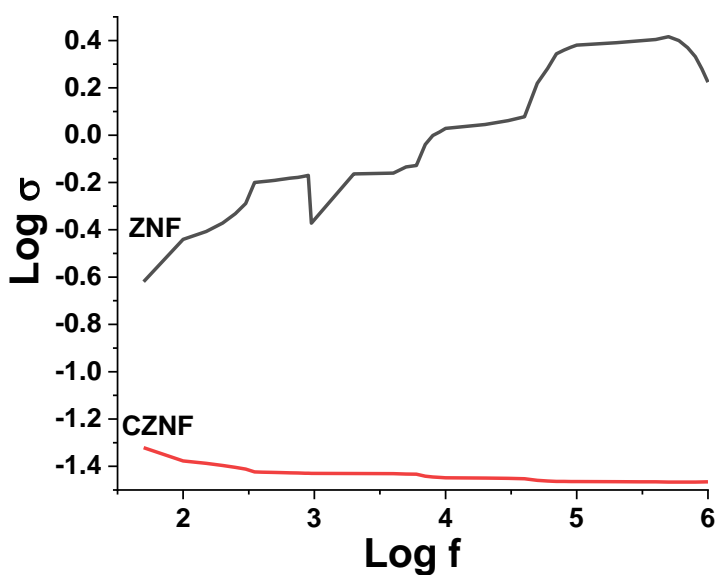


Fig.13: Variation of conductivity of zinc acetate nanofibers (ZNF) and MWCNTs-zinc acetate nanofibers (CZNF).

Antimicrobial Activity

As shown in table (3) Gram positive and negative bacteria were inhibited by compounds CNF2, CNF3, CZNF and CZONF. On the other hand, the tested compounds exhibited different activities against the yeast pathogen *Candidaalbicans* with compounds CNF2, CNF3, CZNF and CZONF. CZNF compound is the most

active against the bacteria and yeast pathogen. So, these compounds can be used as food packaging, baby powder, barrier creams to treat diaper rashes, in Calamine lotion and antidandruff shampoo.

Table 4: Antimicrobial activity of some new compounds

Microorganism	Gram strain reaction	CNF1	CNF2	CNF3	CZNF	CZONF	ZONF	CONTROL (DEMSO)	REFERENCE
<i>Candida albicans</i>		15	15	18	30	25	0.12	15	40
<i>Bacillus cereus</i>	Positive	10	17	10	30	25	10	10	28
<i>Staphylococcus aureus</i>	Positive	15	19	15	36	0	0	15	31
<i>E Escherichia coli</i>	Negative	11	12	12	24	19	10	12	26
<i>Pseudomonas aeruginosa</i>	Negative	11	19	11	25	20	0	12	27

Conclusions:

MWCNTs and MWCNTs/ZnO composite nanofibers were successfully prepared by the electrospinning technique. The spun nanofibers were investigated including morphology, structure, chemical composition, bandgap and transmittance. The deposited nanofibers of ZnO has gained wide spread attention owing to its wide bandgap and high transmittance value. The UV peak at about 300 nm comes from MWCNTs. The peaks at about 368 nm are assigned to UV emission originating from the wide band gap of ZnO. The transmittance value of MWCNTs increased with the addition of ZnO from 56% and 99% in the visible region makes it a candidate for applications in the field of optoelectronics. Electrical properties results showed that the conductivity of ZNF is higher than CZNF, the reason for such low conductivity is that the presence of amorphous carbon and other impurities in MWCNTs prevents the flow of electrons. CZONF nanofibers have electrical properties similar to those of semiconductors and show an electrical conductivity of $5-6 \times 10^2$ S/cm at room temperature. The synthesized nanofibres were studied for antimicrobial activities against the microorganisms. It was observed that the tested compounds CNF2, CNF3, CZNF and CZONF exhibited different activities against the bacteria and yeast pathogen. CZNF compound is the most active against the bacteria and yeast pathogen. So, these compounds can be used as food packaging. It may also be concluded from this study that such nanofibers may be used in pharmaceutical research in future.

Acknowledgements

The authors are thankful to National Research Centre for his fund.



REFERENCES

- [1] Kongkanand A, Kamat PV (2007) Electron storage in single wall carbon nanotubes. Fermi level equilibration in semiconductor–SWCNT suspensions. *ACS Nano* 1(1):13-21. doi:10.1021/nn700036f.
- [2] Kongkanand A, Domy'Onquez RM, Kamat PV (2007) Single wall carbon nanotube scaffolds for photoelectrochemical solar cells: capture and transport of photogenerated electrons. *Nano Lett* 7(3):676-680. doi:10.1021/nl0627238.
- [3] Feynman R. There's plenty of room at the bottom. *J Sci.* 1991;254:1300-1301.
- [4] Sondi I, Salopek-Sondi B. Silver nanoparticles as antimicrobial agent: a case study on E. coli as a model for Gram-negative bacteria. *J Colloid Interface Sci.* 2004;275(1):177.
- [5] Morones JR, Elechiguerra JL, Camacho A, et al. The bactericidal effect of silver nanoparticles. *Nanotechnology.* 2005;16(10):2346.
- [6] Sawai J. Quantitative evaluation of antibacterial activities of metallic oxide powders (ZnO, MgO and CaO) by conductimetric assay. *J Microbial Method.* 2003;54:177-182.
- [7] Loan TT, Long NN, Ha LH. Photoluminescence properties of Co-doped ZnO nanorods synthesized by hydrothermal method. *J Phys D Appl Phys.* 2009;42:65412.
- [8] Akhavan O, Ghaderi E. Enhancement of antibacterial properties of Ag nanorods by electric field. *Sci Tech Adv Mater.* 2009;10:015003-015007.
- [9] Heng TS, Lau SP, Yu SF, et al. Magnetic anisotropy in the ferromagnetic Cu-doped ZnO nanoneedles. *Appl Phys Lett.* 2007;90:032509.
- [10] Zhong CJ, Mave MM. Core Shell assembled nanoparticles as catalysts. *Adv Mater.* 2001;13(19):1507-1511.
- [11] Liz-Marzan LM. Tailoring surface plasmons through the morphology and assembly of metal nanoparticles. *Langmuir.* 2006;22(1):32-41.
- [12] Alammar T, Mudring AV. Facile preparation of Ag/ZnO nanoparticles via photoreduction. *J Material Sci.* 2009;44(12):3218-3222.
- [13] Kawashita M, Tsuneyama S, Miyaji F, Kokubo T, Kozuka H, Yamamoto K. Antibacterial silver-containing silica glass prepared by sol-gel method. *Biomaterials.* 2000;21:393-398.
- [14] Pal S, Tak YK, Song JM. Does the antibacterial activity of silver nanoparticles depend on the shape of the nanoparticle? A study of the Gram-negative bacterium *Escherichia coli*. *J App Environ Microbiol.* 2007;73(6):1712-1720.
- [15] Lin W-C, Chen C-N, Tseng T-T, Wei M-H, Hsieh JH, Tseng WJ. Micellar layer-by-layer synthesis of TiO₂/Ag hybrid :particles for bactericidal and photocatalytic activities. *J Eur Ceram Soc.* 2010;30:2849-2857.
- [16] Kassaei MZ, Akhavan A, Sheikh N, Sodagar A. Antibacterial effects of a new dental acrylic. *J Appl Polym Sci.* 2008;110:1699.
- [17] Lee HJ, Yeo SY, Jeong SH. Antibacterial effect of nanosized silver colloidal solution on textile fabrics. *J Mater Sci.* 2003;38:2199-2204.

- [18] Staumal B, Baretjky B, Mazilkin A, Protasiba S, Petrastrumal A. Increase of Mn solubility with decreasing grain size in ZnO. *J Eur Ceram Soc.* 2009;29:1963.
- [19] Sawai J. Quantitative evaluation of antibacterial activities of metallic oxide powders (ZnO, MgO and CaO) by conductimetric assay. *J Microbial Method.* 2003;54:177-182.
- [20] Loan TT, Long NN, Ha LH. Photoluminescence properties of Co-doped ZnO nanorods synthesized by hydrothermal method. *J Phys D Appl Phys.* 2009;42:65412.
- [21] Akhavan O, Ghaderi E. Enhancement of antibacterial properties of Ag nanorods by electric field. *Sci Tech Adv Mater.* 2009;10:015003-015007.
- [22] Heng TS, Lau SP, Yu SF, et al. Magnetic anisotropy in the ferromagnetic Cu-doped ZnO nanoneedles. *Appl PhysLett.* 2007;90:032509.
- [23] Zhong CJ, Mave MM. CoreShell assembled nanoparticles as catalysts. *Adv Mater.* 2001;13(19):1507-1511.
- [24] Liz-Marzan LM. Tailoring surface plasmons through the morphology and assembly of metal nanoparticles. *Langmuir.* 2006;22(1):32-41.
- [25] E.D. Adelowo, A.Y. Fasasi, M.O. Adeoye, S.O. Alayande, Structural and Optical Properties of Tin Doped Zinc Oxide Fibres Prepared By Electrospinning Technique, *Chemistry and Materials Research* (2013) 96-105.
- [26] X. Zhang, M.R. Reagan, L.K. David, *Electrospun Silk Bio-material Scaffolds for Regenerative Medicine, Advanced DrugDelivery Review* (2009) 988-1006.
- [27] J. -h. He, Y. Liu, *Electrospun Nanofibres and Their Applications*, iSmither, Shrewsbury, 2008.
- [28] W.E. Teo, S. Ramakrishna, A review on electrospinning design and nanofibre assemblies, *Nanotechnology* (2006) R89-R106.
- [29] N. Bhardwaj, S.C. Kundu, *Electrospinning: A fascinating fiber fabrication technique, Biotechnology Advances* 28 (2010) 325-347.
- [30] S. Ramakrishna, K. Fujihara, W.-E. Teo, T.-C. Lim, Z. Ma, *An introduction to electrospinning and nanofibers*, World Scientific Publishing Company Limited, Singapore, 2005.
- [31] B.M. Sorayani, R. Bagherzadeh, M. Latifi, Fabrication of composite PVDF-ZnO nanofiber mats by electrospinning for energy scavenging application with enhanced efficiency, *J Polym Res* 22(130) (2015).
- [32] H.S Bolarinwa, M.U. Onuu, A.Y. Fasasi, S.O. Alayande, L.O. Animasahun, I.O. Abdulsalami, O.G. Fadodun, I.A. Egunjobi Determination of optical parameters of zinc oxide nanofibre deposited by electrospinning technique *Journal of Taibah University for Science* 11 (2017) 1245-1258.
- [33] Wilkins, TD., Holdeman, JJ., Abramson, IJ. and Moore, WEC. 1972. Standardized single-disc method for antibiotic susceptibility testing of anaerobic bacteria. *Antimicrob Agents Chemother.* I. 1(6):451-455.
- [34] S. Martin, G. Liangfeng, T. Satyan, T. Satyanarayana, G. Feng, G. Marc, Simultaneous determination of several crystal structures from powder mixtures: the combination of powder X-ray diffraction, band-target entropy minimization and Rietveld methods, *Journal of Applied Crystallography* 47 (2) (2014) 659-667.
- [35] F. Avilés, J.V. Cauch-Rodríguez, L. Moo-Tah, A. May-Pat, & R. Vargas-Coronado, *47(2009)2970-2975.*

- [36] R. Yudianti, H. Onggo, Y. Saito, T. Iwata, and J.-I. Azuma. Open Materials Science Journal ,vol.5, (2011),pp.242-247.
- [37] Wu, H., Pan, W., 2006. Preparation of Zinc oxide nanofibers by electrospinning. J. Am. Ceram. Soc. 89, 699-701.
- [38] Y.-Y. Cho, C. Kuo, Optical and electrical characterization of elec-trospun Al-doped zinc oxide nanofibers as transparent electrodes, J. Mater. Chem. C 4 (2016) 7649-7657.
- [39] Y. Liao, T. Fukuda, S. Wang, Electrospun metal oxide nanofibers and their energy application, in: M.M. Rahman, M. Abdullah (Eds.), Nanofiber research – Reaching new heights, InTech Open, 2016, pp. 169-190.
- [40] Song SN, Wang XK, Chang RPH, Ketterson JB. Electronic properties of graphite nanotubules from galvanomagnetic effects. Phys Rev Lett, 72, 697 (1994). <http://dx.doi.org/10.1103/PhysRevLett.72.697>.
- [41] Bachtold A, Henny M, Terrier C, Strunk C, Schonberger C, Salvetat JP, Bonard JM, Forro L. Contacting carbon nanotubes selectively with low-ohmic contacts for four-probe electric measurements. Appl Phys Lett, 73, 274 (1998). <http://dx.doi.org/10.1063/1.121778>.
- [42] Dai H, Wong EW, Lieber CM. Probing electrical transport in nanomaterials: conductivity of individual carbon nanotubes. Science, 272, 523 (1996). <http://dx.doi.org/10.1126/science.272.5261.523>.
- [43] Berger C, Yi Y, Wang ZL, de Heer WA. Multiwalled carbon nanotubes are ballistic conductors at room temperature. Appl Phys A, 74, 363 (2002). <http://dx.doi.org/10.1007/s003390201279>.
- [44] Lee RS, Kim HJ, Fischer JE, Thess A, Smalley RE. Conductivity enhancement in single-walled carbon nanotube bundles doped with K and Br. Nature, 388, 255 (1997).
- [45] Randeniya LK, Bendavid A, Martin PJ, Tran CD. Composite yarns of multiwalled carbon nanotubes with metallic electrical conductivity. Small, 6, 1806 (2010). <http://dx.doi.org/10.1002/sml.201000493>.